Simultaneous Volumetric and Functional Right Ventricular Assessment by Principal Strain Analysis in Children with Repaired Tetralogy of Fallot

Article *in* European Heart Journal - Imaging Methods and Practice · May 2025

DOI: 10.1093/ehjimp/qyaf050

CITATIONS
0

READS
15

7 authors, including:

Daisuke Matsubara
The Childrens' hospital of Philadelphia
84 PUBLICATIONS **609** CITATIONS
SEE PROFILE

Renzo JC Calderon-Anyosa
University of Toronto
48 PUBLICATIONS **994** CITATIONS
SEE PROFILE

Anirban Banerjee
The Children's Hospital of Philadelphia
87 PUBLICATIONS **1,192** CITATIONS
SEE PROFILE

ESC European Society of Cardiology

European Heart Journal - Imaging Methods and Practice (2025) **3**, qyaf050
https://doi.org/10.1093/ehjimp/qyaf050

ORIGINAL ARTICLE

Simultaneous volumetric and functional right ventricular assessment by principal strain analysis in children with repaired tetralogy of Fallot

Daisuke Matsubara [1,*†], Ryusuke Numata[1,†], Renzo Calderon-Anyosa[1], Hunter L. Kauffman[1], David M. Biko[2], Gianni Pedrizzetti[3], and Anirban Banerjee[1]

[1]Department of Pediatrics, Division of Cardiology, The Children's Hospital of Philadelphia, Philadelphia, PA 19104, USA
[2]Department of Radiology, The Children's Hospital of Philadelphia, Philadelphia, PA 19104, USA
[3]Department of Engineering and Architecture, University of Trieste, Trieste, TS 34100, Italy

Received 1 February 2025; accepted after revision 1 April 2025; online publish-ahead-of-print 13 May 2025

Abstract

Aims

Principal strain (PS) analysis using 3D speckle-tracking echocardiography enables us to simultaneously measure 3D ventricular volumes and strains. PS quantifies 3D deformation by defining not only amplitude but also direction of principal myocardial contraction (PS angle). This study aims (i) to validate volumetric and functional parameters using PS analysis in volume-overloaded right ventricle (RV) of repaired tetralogy of Fallot (rTOF) vs. cardiac magnetic resonance (CMR) and (ii) to describe PS analysis indices in patients undergoing pulmonary valve replacement (PVR).

Methods and results

Sixty-four paediatric patients with rTOF (12.4 ± 5.2 years) and 58 age-matched healthy children (12.8 ± 3.7 years) were prospectively included. We calculated PS magnitude [global PS (GPS)] and angle, indexed RV end-diastolic and end-systolic volumes (EDVi and ESVi), RV ejection fraction (EF), and conventional strains. Among rTOF patients, 32 CMRs were available. First, we validated volumetric parameters obtained by PS analysis against CMR. Second, we compared these indices between rTOF patients and controls. Lastly, we evaluated the discriminative value of PS analysis in PVR. PS analysis and CMR measurements showed good correlations (EDVi, $r = 0.80$; ESVi, $r = 0.74$; and EF, $r = 0.70$, $P < 0.001$). GPS showed the highest correlation with 3D-EF ($r = -0.84$, $P < 0.001$). rTOF patients exhibited nearly doubled RV volume and significantly decreased 3D-EF and conventional strains. PS magnitude also decreased in rTOF patients, with altered PS angles in RV free wall. Volume measurements of RV showed the highest predictive value for discriminating PVR (+) by receiver operating characteristic analysis, followed by PS functional parameters.

Conclusion

PS analysis is a reliable and reproducible method for both volumetric and functional analysis of volume-overloaded RV in rTOF, which can be of incremental value for defining the indications for PVR.

* Corresponding author. E-mail: 99081dm@jichi.ac.jp
† These authors contributed equally to this work.

Graphical Abstract

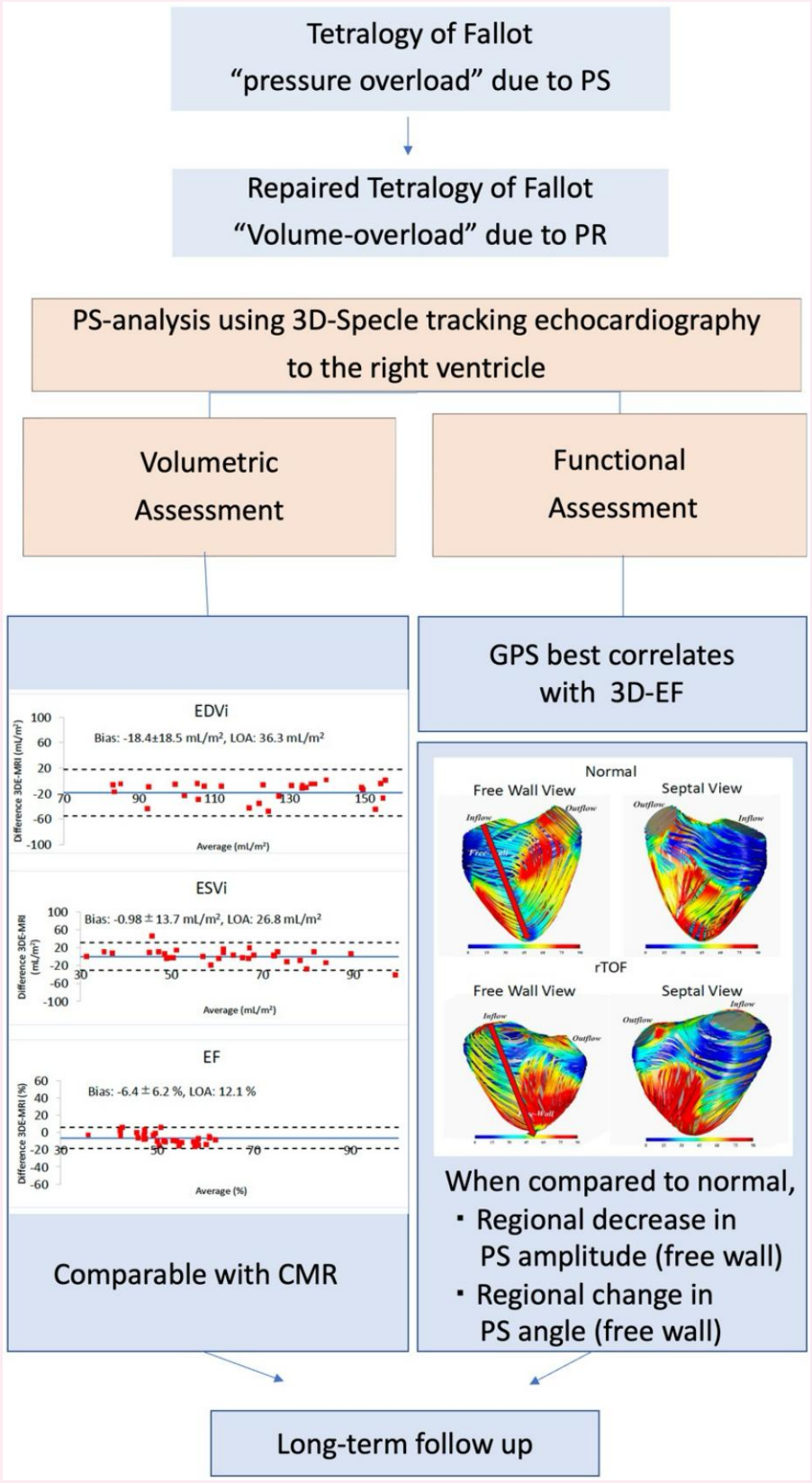

Schematic diagram showing simultaneous volumetric and functional assessment by PS analysis in the volume-overloaded RV of rTOF.

Keywords cardiac magnetic resonance • principal strain analysis • pulmonary valve replacement • right ventricle • tetralogy of Fallot • 3D speckle-tracking echocardiography

Introduction

In patients with tetralogy of Fallot (TOF) repair in early infancy, the right ventricle (RV) may manifest adverse RV remodelling over the years due to dilation secondary to chronic pulmonary regurgitation (PR), electromechanical dyssynchrony, myocardial fibrosis, and gradual functional decline.[1,2] Therefore, quantitative and repeatable assessments of RV volume and function would be advantageous for longitudinal management of repaired TOF (rTOF) patients. However, because of the complex shape of the RV, quantification of RV function and volume using 2D echocardiography has remained a challenge, and RV parameters are often assessed qualitatively (eyeball method) in everyday practice. Semi-quantitative methods, such as tricuspid annular plane systolic excursion, do not provide information on RV volume. Moreover, it is limited to assessing the longitudinal function of only the RV free wall, which is angle dependent and directly influenced by RV volume.[3]

Consequently, measurements of RV volume, pulmonary regurgitant fraction, and RV ejection fraction (RVEF) by cardiac magnetic resonance (CMR) imaging are currently considered as gold standards for clinical decision-making regarding pulmonary valve replacement (PVR).[2] However, CMR imaging is not always practical for frequent assessments during regular outpatient evaluations, particularly in children who often need sedation. In that respect, echocardiography still remains the mainstay of routine clinical follow-up of patients with rTOF. Thus, in rTOF, it is crucial to explore an accurate and reliable echocardiographic method that compares well with CMR for describing both RV volume and functional changes.

More recently, advent of 3D speckle-tracking echocardiography (3D-STE) has allowed us to measure 3D ventricular volumes and 3D strain simultaneously in both left ventricle (LV) and single RV.[4,5] From 3D-STE, a new concept of principal strain (PS) was derived.

Current functional analyses of myocardial deformation by 2D strain provide predominantly geometry-dependent measurements of deformation such as circumferential strain (CS), longitudinal strain (LS), and radial strain. This approach may not realistically represent the 3D nature of the myocardium, where multidirectional sliding motion of the tissue planes, known as 'shear', also occurs throughout the cardiac cycle. Therefore, in the 3D model, there are nine strains, three normal and six shears. As shear strains are difficult to measure, a novel method to overcome this limitation, known as PS, has been proposed using a 3D tensor model. PS analysis eliminates the effects of shear strains because the shear strains are zero, when the concept of a 3D tensor and its eigenvectors are applied to myocardium (*Figure 1*). The corresponding eigenvalue quantifies strain amplitude. Therefore, PS analysis consolidates circumferential, longitudinal, and circumferential–longitudinal shear strains into a single deformation, expressed as PS, and a perpendicular secondary strain (SS).[6,7] Here, PS provides the main measure of contraction yielding, in global terms, a similar information to EF; differently, the SS provides an additional measure of contraction not directly contained in EF.[7] In addition, PS quantifies 3D deformation to define not only the amplitude but also the direction of the principal myocardial contraction (PS angle). PS analysis has been utilized in pressure-overloaded RV of adults with pulmonary hypertension and correlates quite well with clinical severity.[8] However, PS analysis has not been applied to volume-overloaded RV.

Finally, the current prevailing paradigm for PVR is heavily weighted towards pre-PVR measurements of RV volume by CMR, aiming for postoperative normalization of RV size and function in asymptomatic patients to prevent major cardiac events, based on the study by Frigiola *et al.*[2,9,10] However, subsequent studies have questioned this approach. In a group of rTOF patients who were left untreated, Quail *et al.*[11] found no significant deterioration in RV dimensions and function over a median of 1.8 years. Moreover, persistence of RV dilatation in the post-PVR state was not associated with major adverse outcomes. Rather, RV systolic function after PVR was one of the most important independent predictors of serious clinical complications in young adults.[10,12,13]

Therefore, the primary aim of this study was to validate volumetric and functional parameters using PS analysis in volume-overloaded RV of rTOF compared with those from CMR. Secondary, we evaluated the predictive value of PS analysis for discriminating PVR patients with rTOF. We hypothesize that PS analysis will be comparable with CMR and may also provide incremental value for defining the indications for PVR.

Methods

Study design

This is a single-centre, prospective, cross-sectional study.

We prospectively enrolled 64 patients with rTOF who underwent clinically indicated echocardiography at the outpatient clinic of The Children's Hospital of Philadelphia from April 2019 to May 2021 (mean age: 12.4 ± 5.2 years). We excluded patients with rTOF who showed mild RV dilatation and/or mild PR, as evaluated using 2D echocardiography and colour Doppler. Patients with poor image quality were also excluded from the study. In addition, we prospectively enrolled 58 age-matched healthy children with structurally normal hearts as controls (mean age: 12.8 ± 3.7 years). They underwent echocardiography to evaluate benign heart murmurs, chest pain, syncope, or a family history of cardiac disease.

Study procedures

3D echocardiography

3D echocardiographic images of the RV were acquired in full-volume mode by experienced cardiac sonographers using the iE33 ultrasound system (Philips Medical Systems, Andover, MA, USA) or EPIQ CVx ultrasound system (Philips Medical Systems, Andover, MA, USA) with X3-1 or X5-1 matrix array transducers optimized for patient size. 3D full-volume data sets were acquired from RV-focused views, by paying special attention to include the whole free wall and apex of the RV. The 3D data sets consisted of four to six sub-volumes with electrocardiographic gating during breath-holding or quiet breathing at the highest allowable frame rates and were exported to a research workstation at native frame rates. When patients received sedation for CMR, the same level of sedation was maintained during subsequent echocardiography, which was performed in tandem with CMR.

3D-STE and PS analysis

3D-STE was analysed using a commercially available semi-automated software (4D RV-Function 2.0, Image-Arena 4.6.44 software; TomTec Imaging Systems, Munich, Germany). First, endocardial landmarks in RV were manually set. The software automatically tracked the endocardial border throughout the cardiac cycle, generating 3D reconstruction (*Figure 2A*). After careful visual assessment of the tracking quality, manual adjustment of contours was performed if needed.

The coordinate data from endocardial surfaces throughout the cardiac cycle were exported for further processing using custom-built software as previously described.[8] PS magnitude and angle for six segments of RV, as well as SS, were automatically calculated by PS analysis. The RV myocardium was divided into six segments: free wall body/apex, septum body/apex, inflow, and outflow (*Figure 2B*). Along with them, RV end-diastolic and end-systolic volumes (RVEDV and RVESV), RVEF, and other conventional strains (CS and LS) were computed using custom-built software.[8] The volumetric and functional values derived from the custom-built software are almost

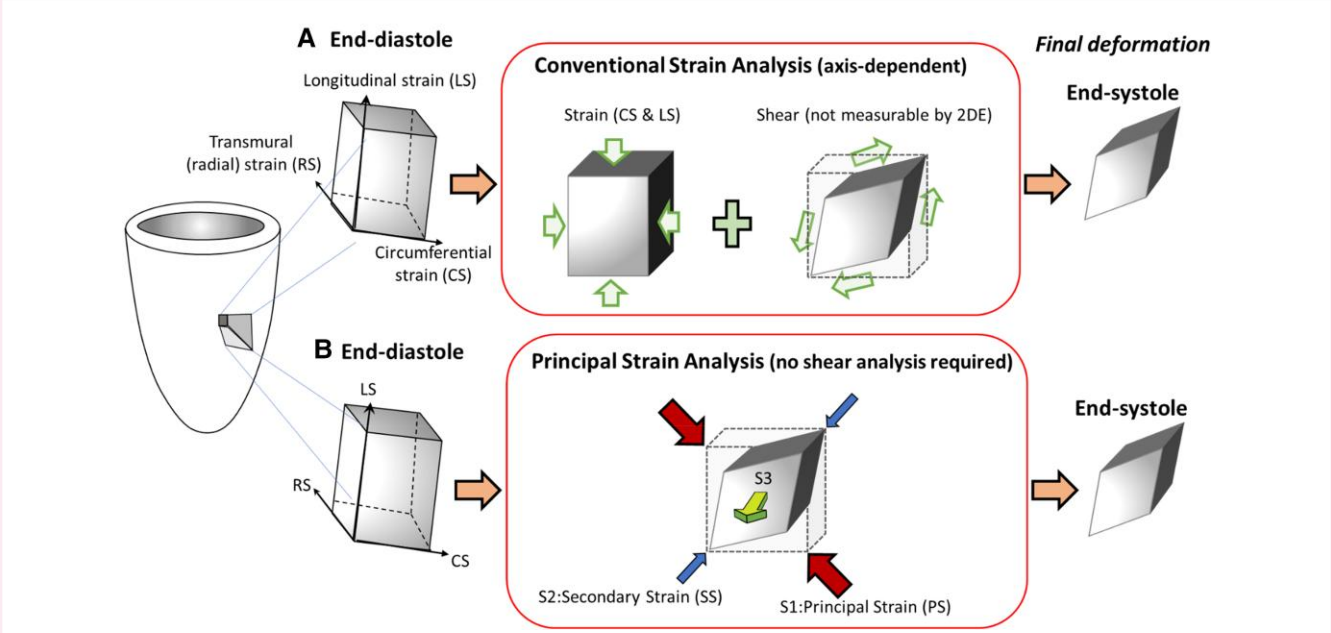

Figure 1 Myocardial tissue deformation. In conventional strain analysis (upper panels), the deformation is evaluated by the geometry-dependent strains (LS, CS, and RS) and shear components, although the shear cannot be measured directly by 2DE. In the PS analysis (lower panels), the deformation was evaluated using three orthogonal eigenvectors, without considering shear components. S1 indicates the dominant contractile force (PS); S2 is the SS, which is orthogonal to PS and has a much lower intensity; and S3 is the positive transmural strain resulting from tissue incompressibility. S3 completely depends on S1 and S2 (S1 + S2 ≈ S3) and can be excluded. Therefore, S1 and S2 can provide a simplified two-component model of myocardial deformation, which is more comprehensive than conventional axis-dependent strains. 2DE, 2D echocardiography; CS, circumferential strain; LS, longitudinal strain; PS, principal strain; RS, radial strain; SS, secondary strain (reprinted with permission from the *Journal of the American Society of Echocardiography*).

identical to those obtained from TomTec software, as they are calculated using mathematical formulas applied to identical contour data. This custom-built software has been extensively validated and utilized in numerous previous studies, both clinical and theoretical.[5–8]

Cardiovascular MRI

We reviewed the CMRs that were closest in time immediately prior to surgical decision-making for PVR. Fifty per cent of the CMR studies were immediately followed by echocardiography on the same day, using the same level of sedation (in patients needing sedation). The rest of CMR studies were performed within a median time gap of 1.9 (0.7–5.7) months. CMR was performed on a 1.5 Tesla Siemens Magnetom Avanto system FIT (Siemens Medical Solutions, Erlangen, Germany), and post-processing was performed using CVI42 software excluding the RV trabeculae from the blood pool during segmentation (Circle Cardiovascular, Version 5, Calgary, Canada). Protocols included acquisition of retrospectively electrocardiogram-gated stack of cine steady-state free precession images in the short axis and four chambers to obtain ventricular volume data for measurement of the RVEDV, RVESV, and RVEF. Short-axis cine images covered the entire ventricle with 20–30 phases per cardiac cycle based on heart rate with a slice thickness adjusted to obtain 12 slices from the atrioventricular valve to the apex with an in-plane resolution of 1.5–2.5 mm and a flip angle of 75–90°. In addition, a through-plane phase-contrast sequence was used for the quantification of forward and reverse flows measured at the main pulmonary artery to calculate pulmonary valve regurgitant fraction (PRF).

Clinical data

Clinical data were abstracted from medical records, including demographic information and New York Heart Association functional classification at the time of echocardiography. In the TOF cohort, the primary diagnosis of TOF and surgical data were recorded. In this cohort, PVR was clinically indicated for 17 patients. Six of the 17 patients were symptomatic and exhibited exercise intolerance. In the absence of symptoms, PVR was performed in patients with (i) significant RV dilatation due to significant PR or (ii) significant outflow tract/conduit obstruction. Significant RV dilatation was defined by CMR results of indexed RVEDV (RVEDVi) > 150 mL/m^2 or RV/LV EDV ratio > 2. Significant PR was defined qualitatively by colour Doppler or CMR results showing PRF > 25%.

Study measures

Primary outcome

The primary outcome included a description of PS analysis volumetric measurements (EDVi, ESVi, and EF) in the volume-overloaded RV of rTOF compared with CMR. In addition, we compared volumetric and functional parameters obtained by PS analysis between patients with rTOF and age-matched normal controls.

Secondary outcome

The secondary outcome included PS analysis in patients with rTOF who were scheduled for PVR [PVR (+) group, $n = 17$] and those who were not [PVR (−) group, $n = 47$].

This study was approved by the Institutional Review Board of The Children's Hospital of Philadelphia, and all participants provided written informed consent before acquiring research images.

Statistical analysis

Baseline characteristics were compared using Fisher's exact test for categorical variables and Student's *t*-test or Wilcoxon's rank-sum test for continuous variables, as appropriate. Normality was assessed using Shapiro–Wilk test. Echocardiographic measurements between two

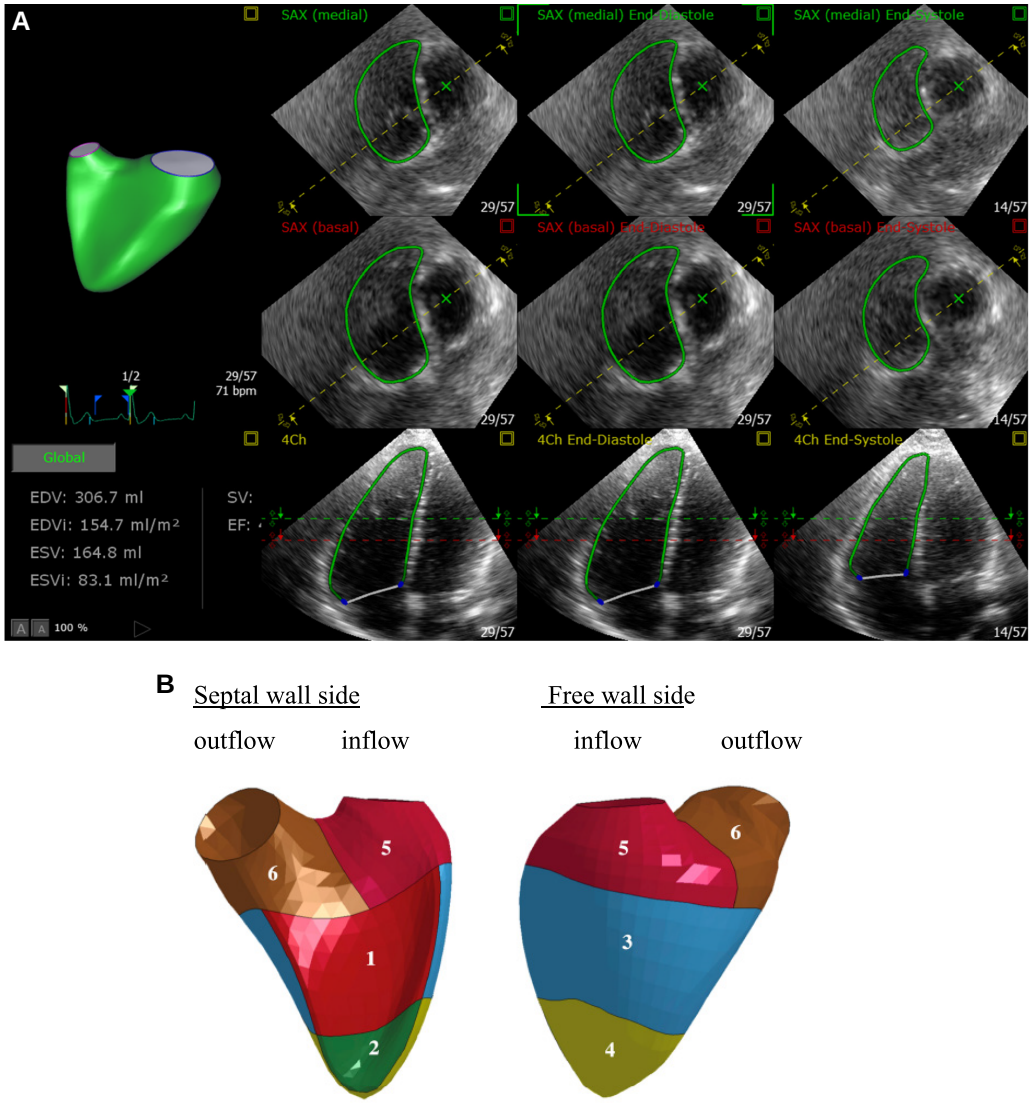

Figure 2 3D-STE (*A*) and six segments of the RV (*B*). The RV is divided into six segments: 1, septal body; 2, septal apex; 3, free wall body; 4, free wall apex; 5, inflow; and 6, outflow segment. EDV, end-diastolic volume; EDVi, indexed end-diastolic volume; EF, ejection fraction; ESV, end-systolic volume; ESVi, indexed end-systolic volume; RV, right ventricle; SV, stroke volume; (reprinted with permission from *Journal of the American Society of Echocardiography*).

independent groups were assessed using two-sample Student's *t*-test or Mann–Whitney *U* test, as appropriate.

Comparison of various measurements between PS analysis and CMR was performed using linear regression and Bland–Altman analysis for bias. The bias was divided by the mean value from CMR to assess the relative difference between the two modalities. Intra-class correlation coefficients (ICCs) were used to evaluate inter-modality agreements between PS analysis and CMR-derived measurements, including EDVi, ESVi, and EF. Two-way mixed-effects models were implemented in ICC with calculation of consistency of agreement, along with 95% confidence intervals (CIs). RVEF and strain measurements using PS analysis were assessed using linear regression with Pearson's correlation coefficients.

To identify variables that differentiate patients with PVR from those with rTOF, univariate logistic regression models were fitted and compared using the Akaike information criterion, with the aim of selecting the most predictive variables. Given the imbalanced nature of the population, the misclassification rate of these models was assessed through 10-fold cross-validation, and the optimal cut-off value was determined by maximizing the *F*1 score to balance precision and recall. The cross-validation estimate of accuracy was also calculated to minimize overfitting and ensure the generalizability of the predictors. The diagnostic accuracy of the optimal predictive variables was further evaluated using receiver operating characteristic (ROC) analyses.

ICCs were also applied to assess intra- and inter-observer reliability of PS analysis-derived measurements, including EDV, ESV, EF, and global PS (GPS). We randomly and blindly selected 15 patients for *de novo* measurements of these parameters by two investigators (H.L.K. and D.M.). For intra-observer reliability, one observer (D.M.) repeated each measurement after 4 weeks.

Statistical significance was defined as a two-tailed $P < 0.05$. Statistical analyses were performed using STATA 15.0 (College Station, TX, USA).

Results

Subject characteristics

Demographic and surgical data are summarized in *Table 1*. Six of the 64 patients (10%) in the rTOF group were symptomatic. All patients with

Table 1 Demographics

Variables	Normal RV ($n = 58$)	rTOF ($n = 64$)	*P*-value
Age at study, years	12.8 ± 3.7	12.4 ± 5.2	0.67
Male, *n* (%)	34 (59%)	31 (48%)	0.36
BSA, m^2	1.4 ± 0.4	1.3 ± 0.4	0.03
Heart rate, bpm	71 ± 14	74 ± 14	0.40
Systolic BP, mmHg	111 ± 12	109 ± 11	0.38
Diastolic BP, mmHg	60 ± 6	63 ± 8	0.02
New York Heart Association classification	I: 58 (100%)	I: 58 (90%)	1.0
	II: 0	II: 6 (10%)	
	III: 0	III: 0	
	IV: 0	IV: 0	
Anatomy of pulmonary valve, *n* (%)	-	Stenosis: 54 (84%)	-
		Atresia: 9 (14%)	
		Absent: 1 (2%)	
Previous palliation before primary repair	-	Modified BT shunt: 2 (3%)	-
Age at primary repair, month	-	2.3 (1.0–4.0)	-
Type of primary repair, *n* (%)	-	Transannular patch: 55 (86%)	-
		RV-PA conduit: 3 (4%)	
		Pulmonary valvotomy: 5 (8%)	
		Monoleaflet valve: 1 (2%)	
Surgical approach for primary repair, *n* (%)	-	Transatrial approach: 4 (6%)	-
		Ventriculotomy: 58 (91%)	
		Unknown: 2 (3%)	
Previous procedures before study	-	Second surgery: 5 (8%)	-
		PTA: 6 (9%)	
		Stent implantation: 15 (23%)	
Underlying disorder	-	22q11.2 deletion: 2 (3%)	-
		12q23.1 deletion: 1 (2%)	
		Down syndrome: 1 (2%)	
		Goldenhar syndrome: 1 (2%)	

Data are expressed as mean ± standard deviation or median (interquartile range) or *n* (%).
ASD, atrial septal defect; BSA, body surface area; BP, blood pressure; BT, Blalock–Taussig; PA, pulmonary artery; PFO, patent foramen ovale; PTA, percutaneous transluminal angioplasty; RV, right ventricle; rTOF, repaired tetralogy of Fallot; VSD, ventricular septal defect.

rTOF underwent primary repair at a median age of 2.3 months. At the time of primary repair, the majority of patients (91%) underwent right ventriculotomy to reconstruct their outflow tract, while the remaining had valve-sparing operations via right atriotomies. Secondary surgery (not PVR) was required in five patients (8%) due to RV dilatation caused by PR ($n = 2$) and stenosis ($n = 3$), at a median age of 6.3 years. All subjects had images suitable for analysis and were therefore included in the study.

Validation of PS analysis vs. CMR in the TOF cohort

CMR imaging was available for 32 (50%) patients with rTOF (*Table 2*). The mean PRF by CMR was 40%. PS analysis and CMR showed good correlations with EDVi ($r = 0.80$, $P < 0.001$), ESVi ($r = 0.74$, $P < 0.001$), and EF ($r = 0.70$, $P < 0.001$) (*Figure 3*). Notably, Bland–Altman analysis showed that PS analysis had a negative bias in all parameters compared with CMR, suggesting mild underestimation of the volumetric and functional indices obtained by PS analysis. The average difference between magnetic resonance imaging (MRI) and PS analysis was 18.4 ± 18.5 mL/m^2 for EDVi, 1.0 ± 13.7 mL/m^2 for ESVi, and 6.4 ± 6.2% for EF (*Figure 4*). The relative difference between the modalities was 13.9%, 1.7%, and 12.0% for EDVi, ESVi, and EF, respectively. Overall, ICC indicated a good correlation of each parameter between PS analysis and CMR [EDVi: ICCs 0.78, (95% CI 0.60–0.89), $P < 0.001$; ESVi: ICCs

Table 2 Comparison of 3D-STE and CMR in the rTOF cohort

Variables	3D-STE ($n = 32$)	CMR ($n = 32$)	*P*-value
RVEDVi, mL/m^2	118 ± 25	136 ± 31	<0.001
RVESVi, mL/m^2	61 ± 16	62 ± 20	0.69
RVEF, %	48 ± 5	55 ± 9	<0.001

Data are expressed as mean ± standard deviation.
3D-STE, 3D speckle-tracking echocardiography; CMR, cardiovascular magnetic resonance; EDVi, indexed end-diastolic volume; EF, ejection fraction; ESVi, indexed end-systolic volume; RV, right ventricle; rTOF, repaired tetralogy of Fallot.

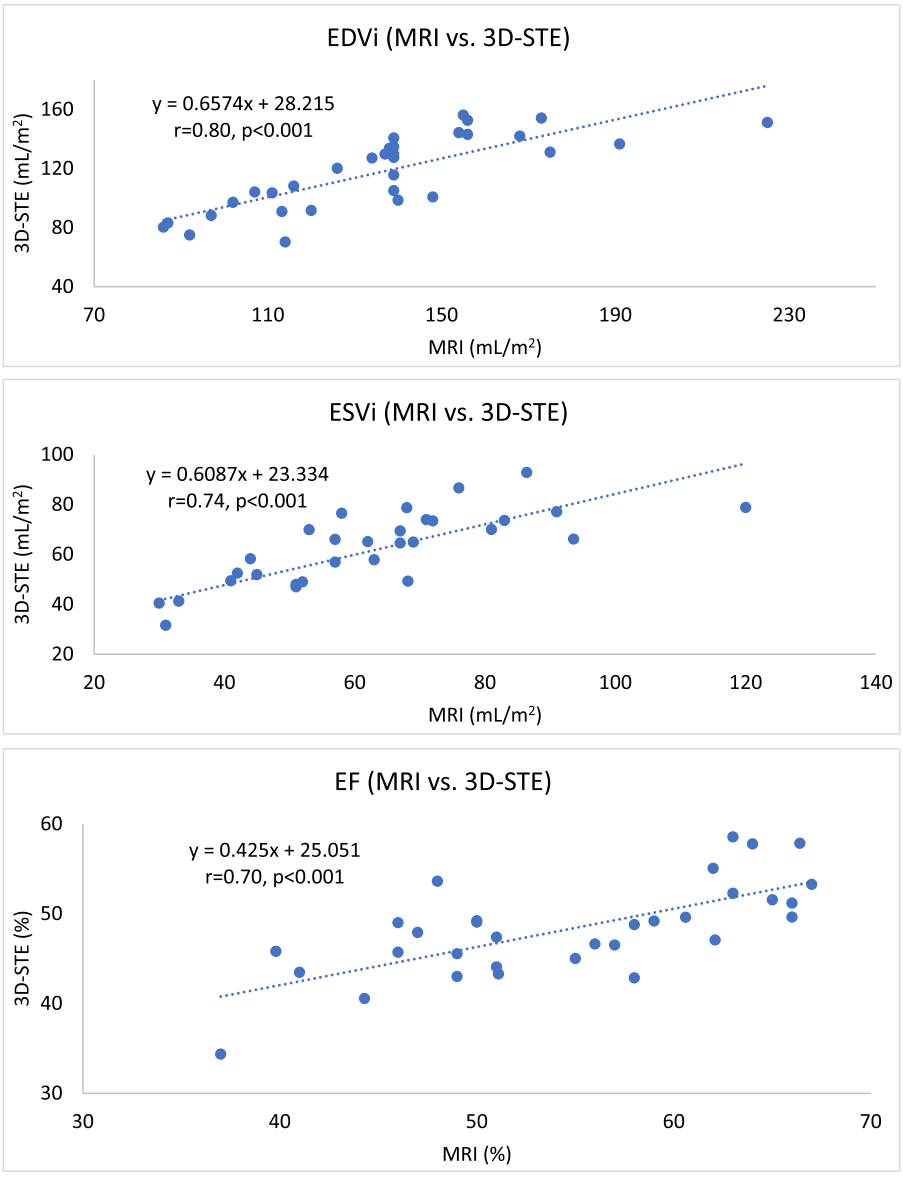

Figure 3 Correlations between PS analysis and CMR in patients with rTOF. PS analysis and CMR showed good correlations in EDVi ($r = 0.80$, $P < 0.001$), ESVi ($r = 0.74$, $P < 0.001$), and EF ($r = 0.70$, $P < 0.001$). 3D-STE, 3D speckle-tracking echocardiography; CMR, cardiovascular magnetic resonance; EDVi, indexed end-diastolic volume; EF, ejection fraction; ESVi, indexed end-systolic volume; MRI, magnetic resonance imaging; rTOF, repaired tetralogy of Fallot.

0.73, (95% CI 0.51–0.86), $P < 0.001$; EF: ICCs 0.62, (95% CI 0.35–0.80), $P < 0.001$].

Comparison of PS analysis parameters between rTOF and normal

When compared with the control group, RV volume in patients with rTOF was almost double (EDVi: 114 ± 22 mL/m^2 vs. 62 ± 12 mL/m^2; ESVi: 58 ± 14 mL/m^2 vs. 27 ± 6 mL/m^2, both $P < 0.001$), and there was a significant decrease in RVEF in rTOF group ($49 \pm 5\%$ vs. $57 \pm 4\%$, $P < 0.001$) (*Table 3*).

Furthermore, rTOF patients showed a significant decrease in magnitude of PS and SS in the global and most of the RV segments, except for the septal body and inflow (*Table 3*). *Figures 5* and *6* show a visual assessment of the PS angle in representative RVs from both control and rTOF patients. In this figure, PS lines in the circumferential direction are 0° (blue lines), while those in the longitudinal direction are 90° (red lines) based on a perpendicular axis from the RV inflow to the apex. PS angle in the normal RV shows circumferential direction, expressed as blue, around the inflow (tricuspid valve), and longitudinal direction, expressed as yellow to red, in the remaining parts (*Figure 5*). The RV of patients with rTOF appears larger and rounder in shape at the apex compared with a normal RV. The PS angle of rTOF patients shows a similar circumferential direction around the inflow (blue), but a more longitudinal direction in the free wall (red), especially at the apex, compared with the normal (*Figure 6*) (also see Supplementary data online, *Videos S1* and *S2* showing rotating images of PS lines). The global PS angle does not differ between the two groups (*Figure 7*).

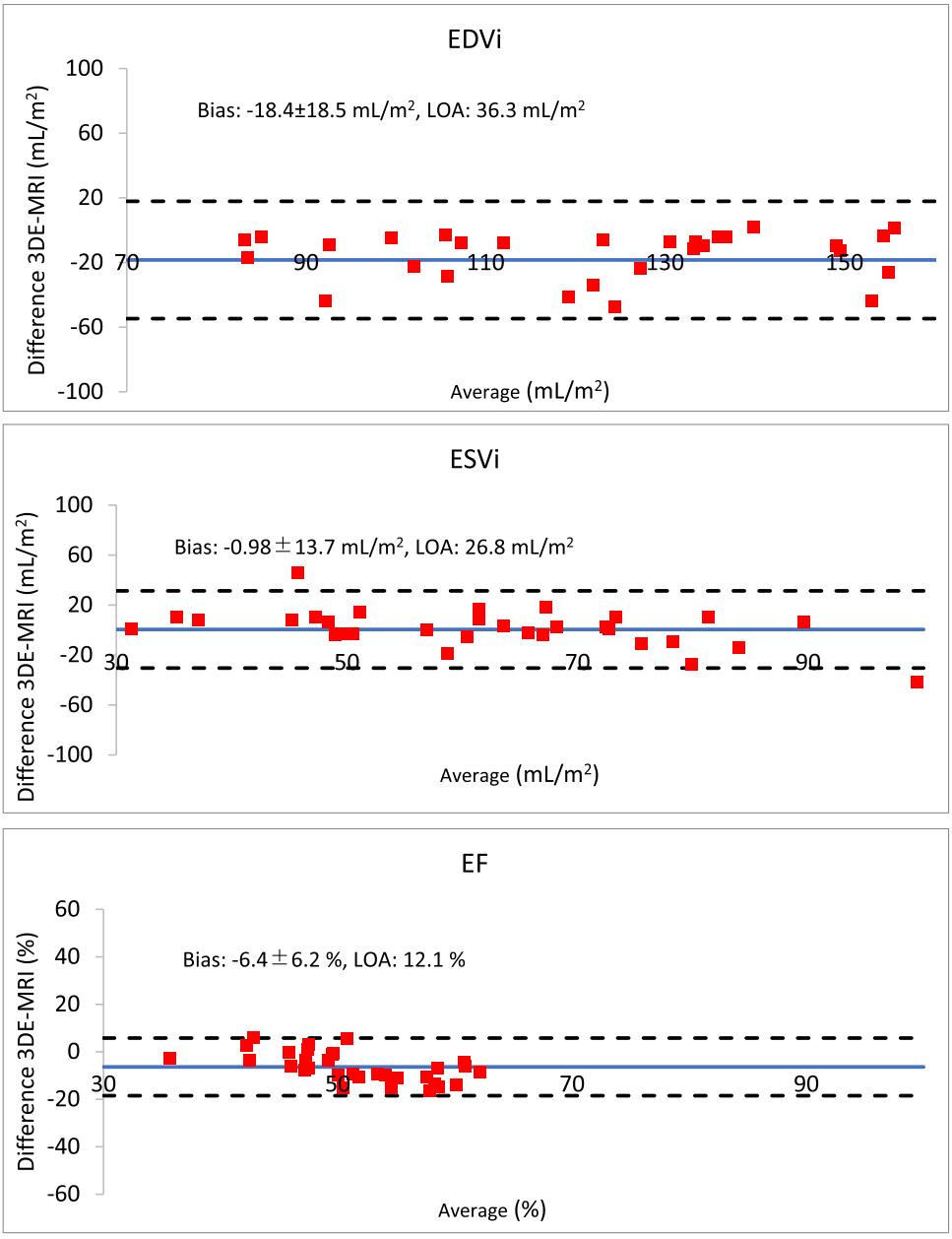

Figure 4 Bland–Altman analysis between PS analysis and CMR in patients with rTOF. Bland-Altman analysis showed that, compared with CMR, PS analysis had a negative bias in all parameters. Notably, the indexed RV end-systolic volume showed only a small bias between the two modalities (bias: 0.48 mL/m^2). The limits of agreement for EF vary with the magnitude of EF, showing an increasing bias at higher EF values and a reduced bias at lower EF values. 3D-STE, 3D speckle-tracking echocardiography; CMR, cardiovascular magnetic resonance; EDVi, indexed end-diastolic volume; EF, ejection fraction; ESVi, indexed end-systolic volume; LOA, limits of agreement; MRI, magnetic resonance imaging; rTOF, repaired tetralogy of Fallot.

Correlation of strains with 3D RVEF

Because of inherent properties of eigenvalues, GPS had a much higher magnitude than other conventional 3D strains in both control and rTOF groups (*Table 3*). GPS showed the best correlation with 3D-EF ($r = -0.84$, $P < 0.001$) among other strains (*Table 4*; *Figure 8*).

PVR (+) and PVR (−) groups in rTOF

There was no difference in age at initial repair between the two groups [PVR (+), $n = 17$; PVR (−), $n = 47$]; however, PVR (+) group was significantly older at the time of echocardiography (*Table 5*). CMR was available in 76% of patients in the PVR (+) group. The PVR (+) group showed significantly larger RV volumes on CMR imaging (median EDVi, 154 mL/m^2 vs. 120 mL/m^2; ESVi, 72 mL/m^2 vs. 53 mL/m^2, $P < 0.001$, respectively). There were no differences in PRF or CMR-RVEF. Similarly, there was a significant difference in EDVi and ESVi by PS analysis (median EDVi 130 mL/m^2 vs. 105 mL/m^2; median ESVi 66 mL/m^2 vs. 54 mL/m^2, both $P < 0.001$), but not in functional measurements, including 3D-EF, conventional strains, and magnitudes of PS and SS.

Table 3 Comparison of PS analysis parameters in the RV between the normal and rTOF groups

Variables	Normal ($n = 58$)	rTOF ($n = 64$)	*P*-value
3D-STE			
Volumes/s	30 ± 7	33 ± 7	0.06
EDVi, mL/m^2	62 ± 12	114 ± 22	<0.001
ESVi, mL/m^2	27 ± 6	58 ± 14	<0.001
EF, %	57 ± 4	49 ± 5	<0.001
GCS, %	−19.7 ± 2.8	−15.0 ± 3.5	<0.001
GLS, %	−15.9 ± 3.0	−12.3 ± 3.2	<0.001
PS (%)			
GPS, %	−30.1 ± 3.2	−26.9 ± 3.9	<0.001
Septal body, %	−33.0 ± 4.8	−32.7 ± 6.8	0.79
Septal apex, %	−41.6 ± 3.9	−33.0 ± 4.6	<0.001
FW body, %	−33.7 ± 6.1	−26.5 ± 7.6	<0.001
FW apex, %	−40.6 ± 5.0	−34.1 ± 4.8	<0.001
Inflow, %	−21.2 ± 4.2	−20.5 ± 8.1	0.42
Outflow, %	−26.0 ± 4.2	−23.3 ± 4.9	0.01
SS (%)			
GSS, %	−5.8 (−8.2 to −3.2)	−0.1 (−4.7 to 2.3)	<0.001
Septal body, %	−13.0 (−15.1 to −10.2)	−6.7 (−9.0 to −2.1)	<0.001
Septal apex, %	−17.5 (−19.6 to −14.6)	−11.7 (−13.7 to −8.1)	<0.001
FW body, %	−11.7 (−14.7 to −10.0)	−3.6 (−7.1 to 0.1)	<0.001
FW apex, %	−17.0 (−18.9 to −13.9)	−11.9 (−15.3 to −10.0)	<0.001
Inflow, %	−3.6 (−5.4 to −0.4)	4.5 (0.1–10.8)	<0.001
Outflow, %	6.7 (1.7–13.0)	10.2 (6.4–15.5)	0.02

Data are expressed as mean ± standard deviation or median (interquartile range).
EDVi, indexed end-diastolic volume; EF, ejection fraction; ESVi, indexed end-systolic volume; FW, free wall; GCS, global circumferential strain; GLS, global longitudinal strain; rTOF, repaired tetralogy of Fallot; SS, secondary strain.

In ROC curves generated to predict PVR, RV volume measurements obtained by PS analysis showed the highest area under the curve (AUC) [EDVi: 0.75, 95% CI (0.62–0.89); ESVi: 0.75, 95% CI (0.61–0.89)], followed by the magnitude of PS in the free wall body [0.62, 95% CI (0.46–0.78)] (*Table 6*; *Figure 9*). In a 10-fold cross-validation, EDVi yielded the highest cross-validation accuracy estimate of 0.78 (with a misclassification error of 21.9%), followed by 0.77 for EF and 0.75 for both ESVi and the magnitude PS in the free wall body (with a misclassification error of 23.4%, 25%, and 25%, respectively; *Table 6*).

Reproducibility

ICCs for intra-observer reliability for EDV, ESV, EF, and GPS by 3D-STE were 0.96, 0.99, 0.98, and 0.94, respectively. ICCs for inter-observer reliability for EDV, ESV, EF, and GPS by 3D-STE were 0.95, 0.94, 0.82, and 0.78, respectively (*Table 7*).

Discussion

This study validates the utility of simultaneous 3DE volumetric and functional analysis utilizing PS in the volume-overloaded RV of children with rTOF. We found that (i) PS analysis is a reliable and reproducible method capable of simultaneously assessing RV volume and function compared with CMR, (ii) GPS showed the highest magnitude of strain and correlated best with 3D-EF among other conventional 3D strains, and (iii) PS analysis demonstrated the distinctive RV mechanics in patients with rTOF compared with normal, showing lower EF and PS magnitude, along with an altered PS angle. In addition, we found that RVESVi as well as RVEDVi derived from PS analysis had clinical utility in discriminating PVR patients, despite an institutional bias towards using RVEDVi for patient scheduled for PVR.

Simultaneous volumetric and functional measurements using PS analysis in rTOF

Although quantitative assessment of RV using echocardiography is challenging, 3DE has been utilized in a few studies in both adults and children.[14–16] A recent study by Li *et al.*[14] in a large number of adults ($n = 174$) with various disease entities showed that RV volumes and EF determined by 3DE strongly correlated with CMR values (EDV: $r = 0.94$; ESV: $r = 0.96$; EF: $r = 0.91$, all $P < 0.001$). However, this study demonstrated a larger bias and wider limit of agreement between 3DE and CMR among patients with lower EF (<45%) or dilated RV (>87 mL/m^2 in men and >74 mL/m^2 in women). Given the severely dilated RV in our cohort, the current study on RV volumes provided excellent data with minimal bias. In addition, our study demonstrated a mild underestimation of RV volume by PS analysis compared with CMR in the dilated RV in diastole, but not in systole, which is consistent with the findings of previous investigator.[16,17] We speculate that poor imaging of the RV free wall and prominent trabeculae in the dilated RV make the identification of the endocardial border difficult, which may lead to a greater underestimation of EDVi by 3DE. However, similar to two previous studies in adults, the ESVi showed a good correlation with CMR-derived values.[16,17] Our results support

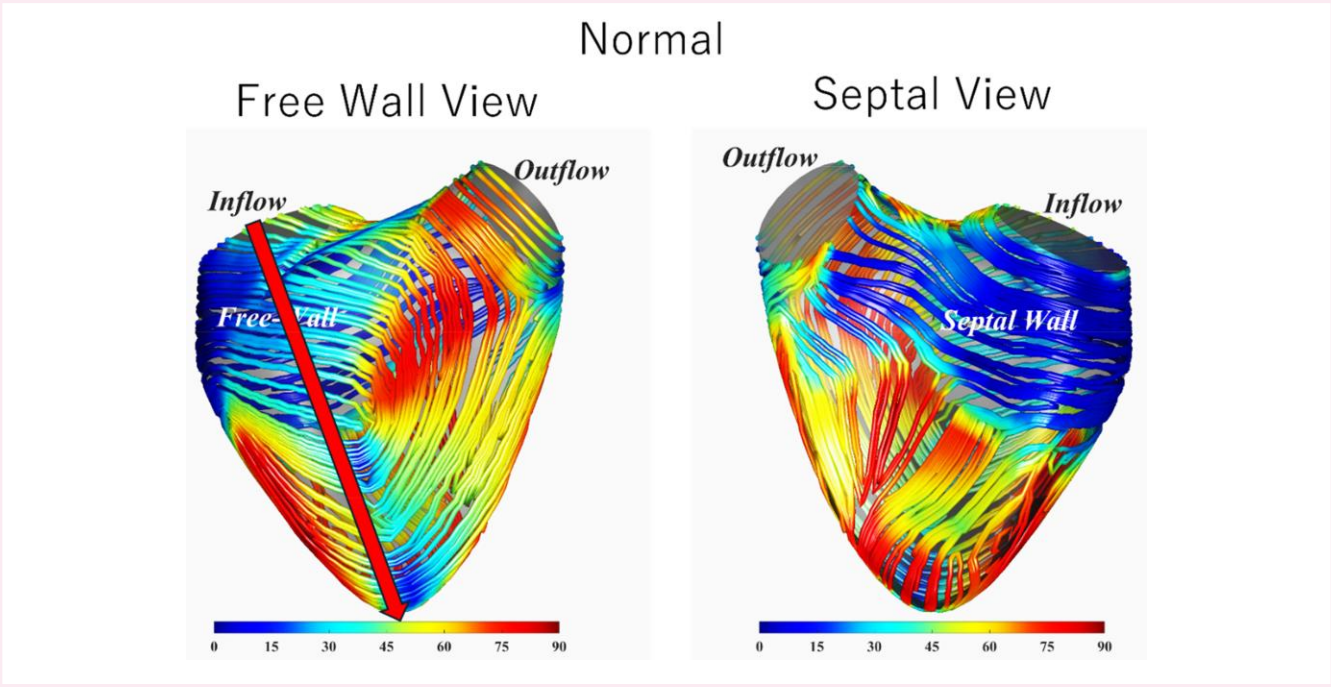

Figure 5 PS angle of the RV in normal subjects. The colour bar represents the PS angle in end-systolic phase, where the long, red arrow indicates a perpendicular axis of the RV extending from inflow to apex. In the normal RV, PS angle shows the circumferential direction (expressed as blue) around the inflow and longitudinal direction (expressed as yellow to red) in the remaining parts.

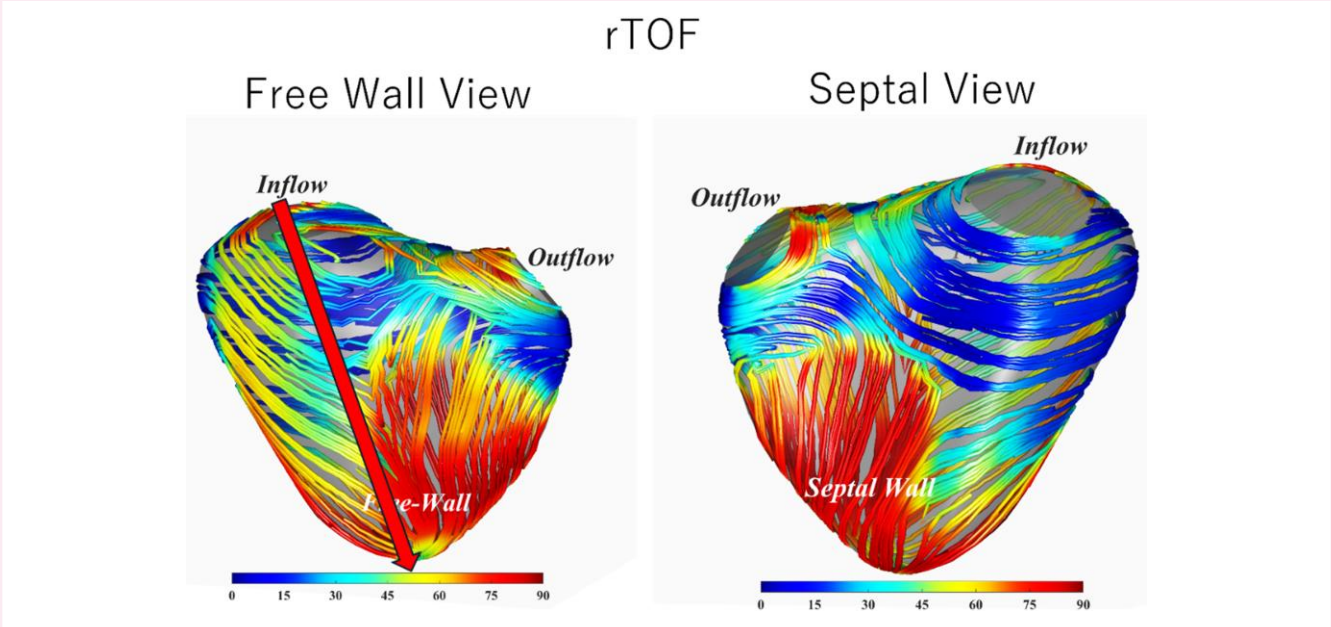

Figure 6 PS angles of the RV in rTOF patients. The long, red arrow indicates a perpendicular axis of the RV, similar to the definition used in normal RVs. In the RV of the rTOF, PS angle shows a similar circumferential direction around the inflow but a more longitudinal direction in the free wall, especially in the apex, compared with the normal RVs (in addition, see Supplementary data online, *Videos S1* and *S2* showing rotating 3D PS line images in RV of normal and rTOF patients, respectively). rTOF, repaired tetralogy of Fallot.

the clinical utility of PS analysis for simultaneous assessment of volume and function of the dilated RV, which is crucial in everyday practice for the long-term management of patients with rTOF. To achieve greater accuracy using PS analysis, the current paradigm of using EDVi may have to be changed to include ESVi as well in making clinical decisions with less bias.

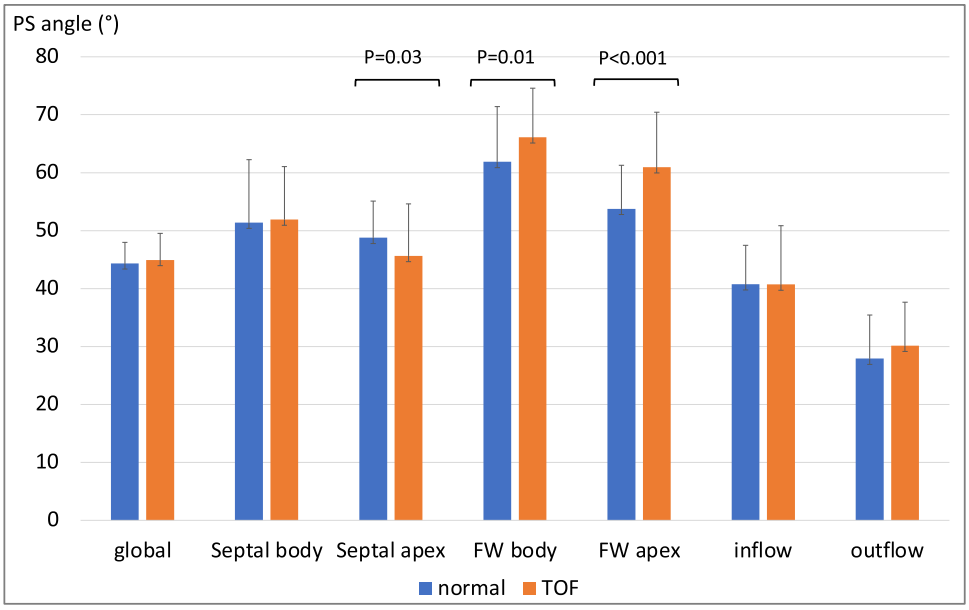

Figure 7 PS angles in normal and rTOF. Although the global PS line does not change between normal and rTOF, the PS line in rTOF is more longitudinal in the RV free wall, especially in the apex, and more circumferential in the septal part than in the normal. FW, free wall; PS, principal strain; TOF, tetralogy of Fallot.

Table 4 Correlation of strains with 3D RVEF

Variables	*r*-value	95% CI	*P*-value
GPS	−0.84	−0.886 to −0.780	<0.001
GCS	−0.71	−0.786 to −0.606	<0.001
GLS	−0.64	−0.736 to −0.522	<0.001

CI, confidence interval; EF, ejection fraction; GCS, global circumferential strain; GLS, global longitudinal strain; GPS, global principal strain; GSS, global secondary strain.

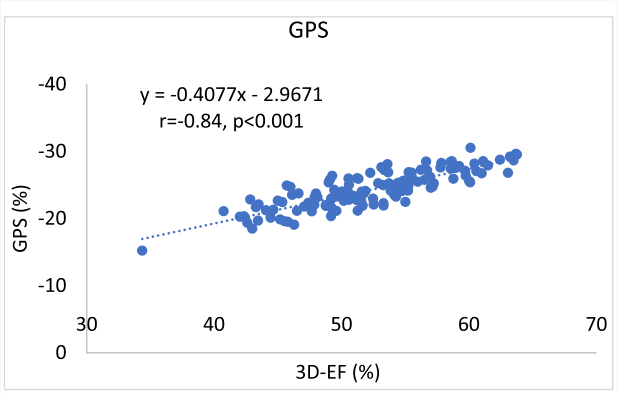

Figure 8 Correlation between GPS and 3D-EF. GPS showed the best correlation with EF by PS analysis among the other strains ($r = -0.84$, $P < 0.001$). 3D-EF, 3D ejection fraction; GPS, global principal strain.

PS analysis of deformation in volume-loaded RV

There is increasing evidence of the incremental value of myocardial deformation imaging in patients with rTOF.[18] Recent advancements in 3D-STE have enabled PS analysis, integrating various conventional strains into a comprehensive deformation assessment without axis dependence.[5] In our study focusing on volume-overloaded RV in rTOF patients, we found that PS was globally impaired in the dilated RV compared with normal subjects. Notably, peak GPS exhibited the highest strain magnitude and correlated most strongly with 3D-EF, consistent with our previous findings in a single RV after Fontan palliation.[5,19]

Another unique feature of PS analysis is that it not only quantifies deformation but also provides insight into the dominant contraction direction via PS angle. If the myocardial tissue was ideally a thin membrane composed of a single sheet of fibres, then the direction of PS would coincide with the direction of the fibres. In real application, the direction of PS angle is read at the endocardium and represents the net result of contraction across the entire myocardial thickness. Therefore, in general, the PS angle represents the dominant direction of contraction produced by the contraction of all fibres in that region. If we can assume that there is a dominant layer of myofibres, the PS angle is an estimation of the direction of these dominant fibres.

In a seminal paper, Sallin[20] has shown elegantly that throughout the cardiac cycle, LVEF depends continuously on the myofibre angle of orientation. Using the concept of tensor similar to that used in our study, experiments on the canine RV have shown the importance of myofibre angle in the RV as well.[21] In our study, PS angle offers a physiological map of deformation patterns, potentially reflecting underlying changes in the myocardium.[6] Acknowledging the constraints of our single-point-in-time study, we speculate that the changes in PS angle may be associated with functional changes or shape changes of the RV in a two-ventricle heart.

We have previously demonstrated that PS analysis in patients with a single RV after Fontan palliation demonstrated a different direction of

Table 5 PS analysis of the PVR (+) and PVR (−) groups in rTOF

Variables	rTOF, PVR (−) ($n = 47$)	rTOF, PVR (+) ($n = 17$)	*P*-value
Age at echocardiogram, years	11.0 (7.7–14.9)	15.7 (11.5–18.6)	<0.01
Age at initial repair, month	2.3 (1.2–4.0)	2.3 (0.6–4.0)	0.60
Duration after initial repair, year	10.2 (7.3–14.1)	15.2 (10.8–18.3)	0.02
New York Heart Association classification	I: 47 (100%)	I: 11 (65%)	<0.001
	II: 0	II: 6 (35%)	
	III: 0	III: 0	
	IV: 0	IV: 0	
Indication for PVR		Symptom: 6 (35%)	
		Dilated RV due to PI: 9 (53%)	
		Dilated RV with PI and stenosis: 2 (12%)	
CMR	($n = 19$)	($n = 13$)	
EDVi, mL/m^2	120 (109–139)	154 (139–173)	<0.001
ESVi, mL/m^2	53 (42–67)	72 (62–86)	0.001
EF, %	57 (51–64)	50 (46–59)	0.23
PRF, %	41 (38–45)	41 (37–49)	0.25
PS analysis			
EDVi, mL/m^2	105 (92–127)	130 (122–142)	<0.001
ESVi, mL/m^2	54 (47–64)	66 (62–73)	<0.001
EF, %	49 (46–52)	49 (46–49)	0.52
GPS	−26.3 (−28.9 to −24.3)	−26.4 (−30.4 to −25.3)	0.99
GSS	2.9 (−3.4 to 3.4)	−0.6 (−5.7 to 1.0)	0.11
GCS	−14.7 (−16.3 to −12.9)	−15.7 (−17.6 to −13.2)	0.51
GLS	−11.6 (−13.8 to −9.9)	−13.3 (−14.2 to −11.0)	0.22
Segmental PS (%)			
Septal body	−33.3 (−37.4 to −28.0)	−34.7 (−36.6 to −32.3)	0.58
Septal apex	−32.3 (−35.6 to −30.1)	−33.4 (−36.4 to −29.6)	0.91
FW body	−27.3 (−33.0 to −23.6)	−22.8 (−28.5 to −19.6)	0.13
FW apex	−34.5 (−36.4 to −31.7)	−34.0 (−35.9 to −32.6)	0.89
Inflow	−18.2 (−23.1 to −14.9)	−19.0 (−23.4 to −17.1)	0.49
Outflow	−23.3 (−27.7 to −20.1)	−21.9 (−24.9 to −19.5)	0.77
Segmental SS (%)			
Septal body	−6.4(−8.9 to −1.6)	−7.1 (−9.9 to −5.6)	0.23
Septal apex	−11.5 (−13.7 to −8.0)	−12.0 (−13.7 to −8.2)	0.50
FW body	−3.3 (−7.1 to 1.1)	−3.8(−5.4 to 1.7)	0.64
FW apex	−11.8 (−15.2 to −9.4)	−12.1 (−16.4 to −11.1)	0.37
Inflow	4.5 (0.2–13.0)	4.1 (0.6–8.0)	0.37
Outflow	11.0 (7.8–16.5)	8.7 (0.9–13.3)	0.21
Exercise test	($n = 13$)	($n = 8$)	
Predicted peak VO_2 (%)	89 (68–103)	79 (65–107)	0.78
Predicted AT (%)	93 (75–106)	105 (80–117)	0.90

Data are expressed as median (interquartile range).
CI, confidence interval; CMR, cardiac magnetic resonance; EDVi, indexed end-diastolic volume; EF, ejection fraction; ESVi, indexed end-systolic volume; FW, free wall; GCS, global circumferential strain; GLS, global longitudinal strain; GPS, global principal strain; PS, principal strain; PVR, pulmonary valve replacement; rTOF, repaired tetralogy of Fallot; SS, secondary strain.

the PS angle in each segment.[19] In addition, the global PS angle in single RV patients was in between the normal LV (circumferential direction) and normal RV (longitudinal direction), suggesting an insufficient compensation in a single RV in mimicking the LV. Similarly, another study on pressure-overloaded RV in adults with idiopathic pulmonary hypertension revealed changes in PS angle from oblique angle to more circumferential orientation correlating with disease progression, indicating prognostic value of PS analysis in this cohort.[8]

The present study on volume-overloaded RV in rTOF patients described an altered PS angle, especially in the free wall apex, showing a shift towards a more longitudinal direction, compared with normal RVs ($60.9 \pm 9.5°$ vs. $53.8 \pm 7.5°$, $P < 0.05$) (*Figures 5–7*). To date, the regional mechanics of the RV have not been fully investigated owing to the unique geometry of the RV. However, the RV free wall, especially the apical segment, in rTOF may play an essential role in maintaining RV function. Previous studies using 2D deformation images in rTOF both

Table 6 ROC curves for discriminating PVR (+) patients in rTOF using PS analysis

Variables	AUC (95% CI)	Cut-off value	Specificity (%)	Sensitivity (%)	cv accuracy (%)	Misclassification error (%)
3D-EDVi	0.753 (0.616–0.891)	120.1 (mL/m^2)	70.2	76.5	78.1	21.9
3D-ESVi	0.751 (0.611–0.891)	64.5 (mL/m^2)	76.6	70.6	75.0	25.0
GSS	0.626 (0.473–0.779)	−0.6 (%)	51.1	64.7	76.6	23.4
PS, FW body	0.619 (0.461–0.777)	−22.8	78.7	52.9	75.0	25.0
GLS	0.605 (0.447–0.760)	−12.5	59.6	64.7	73.4	26.6
GCS	0.570 (0.399–0.740)	−15.4	59.6	58.8	73.4	26.6
3D-EF	0.559 (0.393–0.726)	49.2	48.9	76.5	76.6	23.4
GPS	0.540 (0.368–0.713)	−26.4	51.1	54.7	73.4	26.6
MRI-EDVi	0.810 (0.646–0.975)	148.0 (mL/m^2)	90.0	66.7	81.2	18.8
MRI-ESVi	0.776 (0.604–0.949)	62.0 (mL/m^2)	63.2	75.2	81.2	18.8
MRI-EF	0.623 (0.415–0.831)	50 (%)	70.0	50.0	71.9	28.1

AUC, area under the curve; CI, confidence interval; cv-accuracy, cross-validation accuracy; EDVi, indexed end-diastolic volume; EF, ejection fraction; ESVi, indexed end-systolic volume; FW, free wall; GCS, global circumferential strain; GLS, global longitudinal strain; GPS, global principal strain; rTOF, repaired tetralogy of Fallot; GSS, global secondary strain.

in adults and children showed that RV apical longitudinal deformation was most affected among other RV segments and correlated best with exercise capacity.[22,23] Also, in TOF patients, it has been shown both by CMR and 3DE that the apical EF was the most important contributor to the increased output.[24,25] Compared with the normal RV, where longitudinal force is the major contractile direction, the rTOF in the present study showed a more longitudinal direction in the free wall apex, which could serve as a compensating mechanism. The finding that only 10% of rTOF patients in the present study exhibited symptoms (New York Heart Association functional classification: Stage II) despite their significantly dilated RV volume, compared with normal, may support this hypothesis. In addition, electromechanical dyssynchrony is worth highlighting to understand the pathophysiology of progressive RV dysfunction in rTOF. Friedberg *et al.*[26] demonstrated abnormal RV segmental interactions in rTOF using 2D echocardiographic strain. The septum shows early activation, whereas the lateral RV undergoes early pre-stretching and late activation, resulting in post-systolic shortening. This pattern is typical of the RV in rTOF compared with healthy controls.[26] We speculate that these segmental differences between the septum and the lateral wall may be reflected in the changes in PS angles observed in the present study.

In this context, morphologic studies are also worthy of consideration. In a classical morphological study of RV myoarchitecture in explanted TOF specimens, Sanchez-Quintana *et al.* showed that the superficial layer had a more oblique myofibre orientation in TOF than the normal RV. In the deep layers, myofibres had a longitudinal arrangement in TOF.[27] They showed that the inherent myofibre architecture in the RV of TOF is different from that of the normal RV. This myofibre difference could be reflected by the directional change in the PS lines in rTOF.

PS analysis to refine the indications for PVR

Almost 20 years ago, Frigiola *et al.* proposed a PVR policy that relied on a cut-off value for RVEDVi of 150 mL/m^2. Their study showed that at this threshold value, PVR leads to the normalization of RV volumes, improvement in biventricular function, and submaximal exercise capacity after the repair.[2] However, a subsequent study by the same group could not identify an absolute ceiling beyond which PVR could not normalize the RV dimensions.[11] Nevertheless, there is significant emphasis on RV diastolic volume when making decisions for PVR.[2,28] Therefore, in the present study, the conventional cut-off for RVEDVi would introduce an inherent selection bias in our PVR group.

Several studies have shown a reduction in RV volume and a subjective improvement in exercise capacity after PVR.[2,9] At the same time, in a study on 100 consecutive rTOF patients undergoing CMR at a median follow-up period of 21 years after repair, Geva *et al.* have shown that degree of PR and RVEDVi was not associated with impaired clinical status. Instead, severe RV systolic dysfunction was the strongest independent factor associated with poor clinical status in long-term survivors of rTOF.[29] Therefore, in addition to volume assessment, functional measurements are required to determine the optimal timing for PVR.

Our study cannot answer the question of whether PVR should be performed at a lower or higher predetermined RVEDVi (e.g. 150 mL/m^2). However, we achieved our primary goal and performed

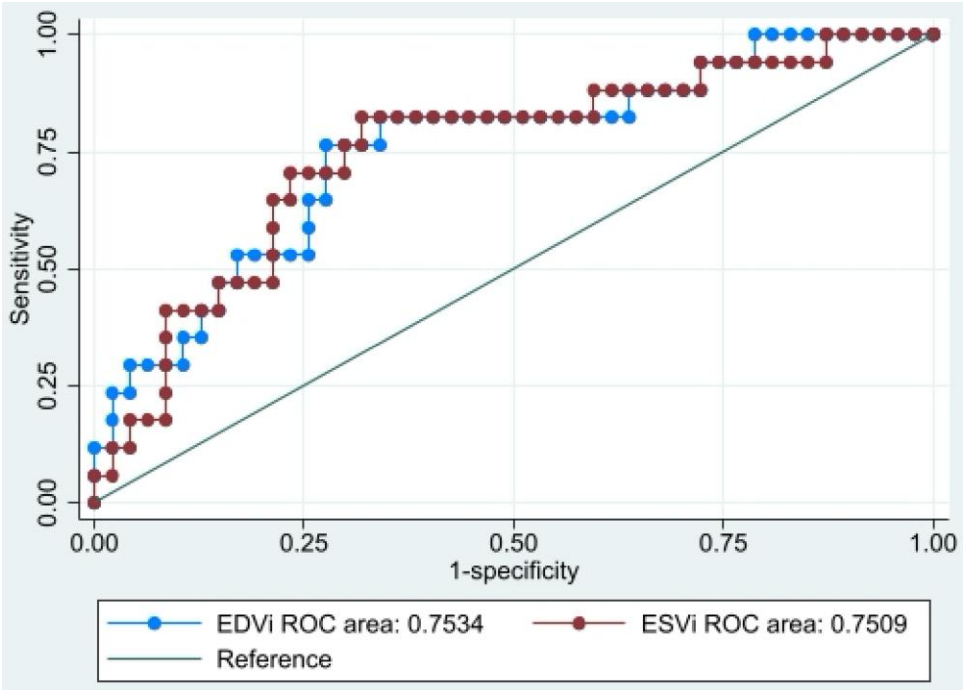

Figure 9 ROC to identify those scheduled for PVR among rTOF patients. RV volume measurements obtained by PS analysis showed the highest AUC. There were no significant differences in AUC between EDVi and ESVi (see Results section for cut-off values). AUC, area under the curve; EDVi, indexed end-diastolic volume; ESVi, indexed end-systolic volume; ROC, receiver operating characteristic.

Table 7 Reliability of PS analysis expressed by intra- and inter-observer variability

			P-value	Bias (95% LOA)	ICCs
Inter-observer variability	Observer 1 (D.M.)	Observer 2 (H.L.K.)			
RVEDVi (mL)	113.8 (70.9, 136.0)	105.5 (68.5, 126.6)	<0.0001	4.34 (−8.214 to 16.894)	0.95
RVESVi (mL)	57.2 (31.8, 71.1)	53.0 (32.5, 64.2)	<0.0001	2.8 (−5.124 to 10.724)	0.94
RVEF (%)	49.7 (47.3, 53.3)	49.8 (48.3, 53.0)	<0.0001	−0.307 (−3.972 to 3.359)	0.82
GPS (%)	−23.2 (−24.7, −21.1)	−24.9 (−26.6, −23.5)	0.0002	1.827 (−1.950 to 5.604)	0.78
Intra-observer variability	First	Second			
RVEDVi (mL)	113.8 (70.9, 136.0)	118.8 (72.1, 135.0)	<0.0001	0.967 (−10.670 to 12.604)	0.96
RVESVi (mL)	57.2 (31.8, 71.1)	57.3 (31.1, 70.0)	<0.0001	0.220 (−7.876 to 8.316)	0.99
RVEF (%)	49.7 (47.4, 53.3)	49.6 (46.6, 54.6)	<0.0001	−0.313 (−4.727 to 4.100)	0.98
GPS (%)	−23.2 (−24.7, −21.1)	−22.8 (−25.7, −22.0)	<0.0001	1.194 (−2.581 to 4.969)	0.94

Data are expressed as median (interquartile range).
EDVi, indexed end-diastolic volume; EF, ejection fraction; ESVi, indexed end-systolic volume; GPS, global principal strain; ICCs, intra-class correlation coefficients; LOA, limits of agreement; RV, right ventricle.

a PS analysis validation study, where RVEDVi was underestimated by 18.4 mL/m^2 but RVESVi was similar to the CMR-derived values. In addition, our study demonstrated the clinical utility of RVESVi as well as RVEDVi in differentiating patients with PVR (+). Our results and several previous studies call for a possible shift in the currently prevailing paradigm and utilize RVESVi (along with RVEDVi) for the longitudinal follow-up of rTOF patients in the clinical setting.[16] Thus, PS analysis may be adequate to monitor serial changes in dilated RV on a more frequent basis in everyday practice and may complement the application of serial cardiac MRI performed less frequently. Moreover, despite showing no functional difference in both the PVR (+) and PVR (−) groups, regional PS analysis, especially in the RV free wall, could potentially provide us with additional information for the indication of PVR. The current study, utilizing PS analysis, introduces a new measure of function that may provide new insights into the assessment of this patient group, particularly where the timing of PVR remains uncertain.

Limitations

This was a cross-sectional study that could not answer the question regarding the optimal timing of PVR and its association with adverse events. A longitudinal study at several time points before and after

PVR is needed to study the clinical outcomes of early vs. late PVR. This was beyond the scope of the present study. Furthermore, the indications for PVR were not standardized in our cohort and may suffer from institutional bias towards RVEDVi in pursuing PVR. In addition, the evaluation of the LV using PS analysis may offer a better understanding of the RV–LV interaction in rTOF. The acquisition of simultaneous 3DE of the LV was beyond the primary goal of our study and, therefore, was not performed. Finally, this was a single-centre study with a small number of patients. The PVR (+) patients were significantly older than PVR (−) patients, which might confound these findings. We propose that a larger number of patients should be studied to confirm the utility of PS analysis in defining the indications for PVR and risk stratification.

Conclusions

This was the first study to apply PS analysis to volume-overloaded RV in children. The volumetric analysis of the dilated RV of rTOF by PS analysis was comparable with that by CMR, with RVESVi showing the best correlation. In addition, concurrent functional analysis demonstrated the distinctive segmental differences in the RV in patients with rTOF compared with normal, showing lower PS magnitude and an altered PS angle, which may provide new insights into the assessment of optimal timing of PVR. A larger longitudinal study without entry bias may enhance the utility of PS analysis in this patient cohort. We speculate that simultaneous RV volumetric and functional assessments by PS analysis may be of incremental value for long-term follow-up of this group of patients and for defining the indications for PVR.

Acknowledgements

No involvement of artificial intelligence programmes in the present study.

Supplementary data

Supplementary data are available at European Heart Journal - Imaging Methods and Practice online.

Consent

All participants provided written informed consent before acquiring research images.

Funding

This research did not receive any specific grant from funding agencies in the public, commercial, or not-for-profit sectors.

Conflict of interest: None declared.

Data availability

The data underlying this article will be shared on reasonable request to the corresponding author.

Authors' contributions

All authors contributed to this research and the preparation of the article. D.M. and R.N. led the research and wrote the manuscript. R.C.-A. interpreted the data from a statistical perspective. H.L.K. performed the STE and PS analyses. D.M.B., G.P., and A.B. supervised the research and critically revised the manuscript. All authors have approved the final version of the article.

Lead author biography

Dr Daisuke Matsubara is a board-certified paediatric cardiologist in Japan with specialized expertise in echocardiography, working at Jichi Medical University. This study was conducted at the Children's Hospital of Philadelphia, where he served as an international research associate. His research interests focus on cardiac functional assessment in paediatric heart diseases, with a particular emphasis on myocardial strain and other advanced echocardiographic techniques.

Ryusuke Numata, MD, PhD, is a research fellow in the Division of Cardiology at the Children's Hospital of Philadelphia, United States. He also serves as Chief Physician in the Department of Paediatric Cardiology at Nagano Children's Hospital in Japan. His research focuses on evaluating cardiac function using 2D or 3D speckle-tracking echocardiography in patients with congenital heart disease.

References

1. Babu-Narayan SV, Kilner PJ, Li W, Moon JC, Goktekin O, Davlouros PA *et al.* Ventricular fibrosis suggested by cardiovascular magnetic resonance in adults with repaired tetralogy of Fallot and its relationship to adverse markers of clinical outcome. *Circulation* 2006;**113**:405–13.
2. Frigiola A, Redington AN, Cullen S, Vogel M. Pulmonary regurgitation is an important determinant of right ventricular contractile dysfunction in patients with surgically repaired tetralogy of Fallot. *Circulation* 2004;**110**:II153–7.
3. Mercer-Rosa L, Parnell A, Forfia PR, Yang W, Goldmuntz E, Kawut SM. Tricuspid annular plane systolic excursion in the assessment of right ventricular function in children and adolescents after repair of tetralogy of Fallot. *J Am Soc Echocardiogr* 2013;**26**:1322–9.
4. Flu W-J, van Kuijk J-P, Bax JJ, Gorcsan J, Poldermans D. Three-dimensional speckle tracking echocardiography: a novel approach in the assessment of left ventricular volume and function? *Eur Heart J* 2009;**30**:2304–7.
5. Sato T, Calderon RJ, Klas B, Pedrizzetti G, Banerjee A. Simultaneous volumetric and functional assessment of the right ventricle in hypoplastic left heart syndrome after Fontan palliation, utilizing 3-dimensional speckle-tracking echocardiography. *Circ J* 2020;**84**:235–44.
6. Pedrizzetti G, Kraigher-Krainer E, De Luca A, Caracciolo G, Mangual JO, Shah A *et al.* Functional strain-line pattern in the human left ventricle. *Phys Rev Lett* 2012;**109**:048103.
7. Pedrizzetti G, Sengupta S, Caracciolo G, Park CS, Amaki M, Goliasch G *et al.* Three-dimensional principal strain analysis for characterizing subclinical changes in left ventricular function. *J Am Soc Echocardiogr* 2014;**27**:1041–50.e1.
8. Satriano A, Pournazari P, Hirani N, Helmersen D, Thakrar M, Weatherald J *et al.* Characterization of right ventricular deformation in pulmonary arterial hypertension using three-dimensional principal strain analysis. *J Am Soc Echocardiogr* 2019;**32**:385–93.
9. Oosterhof T, van Straten A, Vliegen HW, Meijboom FJ, van Dijk APJ, Spijkerboer AM *et al.* Preoperative thresholds for pulmonary valve replacement in patients with corrected tetralogy of Fallot using cardiovascular magnetic resonance. *Circulation* 2007;**116**:545–51.
10. Geva T. Repaired tetralogy of Fallot: the roles of cardiovascular magnetic resonance in evaluating pathophysiology and for pulmonary valve replacement decision support. *J Cardiovasc Magn Reson* 2011;**13**:9.
11. Quail MA, Frigiola A, Giardini A, Muthurangu V, Hughes M, Lurz P *et al.* Impact of pulmonary valve replacement in tetralogy of Fallot with pulmonary regurgitation: a comparison of intervention and nonintervention. *Ann Thorac Surg* 2012;**94**:1619–26.

12. Pastor TA, Geva T, Lu M, Duarte VE, Drakeley S, Sleeper LA *et al.* Relation of right ventricular dilation after pulmonary valve replacement to outcomes in patients with repaired tetralogy of Fallot. *Am J Cardiol* 2020;**125**:977–81.
13. Harrild DM, Berul CI, Cecchin F, Geva T, Gauvreau K, Pigula F *et al.* Pulmonary valve replacement in tetralogy of Fallot: impact on survival and ventricular tachycardia. *Circulation* 2009;**119**:445–51.
14. Li Y, Zhang L, Gao Y, Wan X, Xiao Q, Zhang Y *et al.* Comprehensive assessment of right ventricular function by three-dimensional speckle-tracking echocardiography: comparisons with cardiac magnetic resonance imaging. *J Am Soc Echocardiogr* 2021;**34**:472–82.
15. Yu H-k, Li S-j, Ip JJK, Lam WWM, Wong SJ, Cheung Y-f. Right ventricular mechanics in adults after surgical repair of tetralogy of Fallot: insights from three-dimensional speckle-tracking echocardiography. *J Am Soc Echocardiogr* 2014;**27**:423–9.
16. Ishizu T, Seo Y, Atsumi A, Tanaka YO, Yamamoto M, Machino-Ohtsuka T *et al.* Global and regional right ventricular function assessed by novel three-dimensional speckle-tracking echocardiography. *J Am Soc Echocardiogr* 2017;**30**:1203–13.
17. van der Zwaan HB, Helbing WA, McGhie JS, Geleijnse ML, Luijnenburg SE, Roos-Hesselink JW *et al.* Clinical value of real-time three-dimensional echocardiography for right ventricular quantification in congenital heart disease: validation with cardiac magnetic resonance imaging. *J Am Soc Echocardiogr* 2010;**23**:134–40.
18. Li VW-Y, Yu CK-M, So EK-F, Wong WH-S, Cheung Y-F. Ventricular myocardial deformation imaging of patients with repaired tetralogy of Fallot. *J Am Soc Echocardiogr* 2020;**33**:788–801.
19. Sato T, Matsubara D, Wang Y, Agger P, Pedrizzetti G, Banerjee A. Contraction patterns of post-Fontan single right ventricle versus normal left and right ventricles in children: insights from principal strain analysis. *J Am Soc Echocardiogr* 2023;**36**:878–87.
20. Sallin EA. Fiber orientation and ejection fraction in the human left ventricle. *Biophys J* 1969;**9**:954–64.
21. Meier GD, Ziskin MC, Bove AA. Helical fibers in myocardium of dogs change their pitch as they contract. *Am J Physiol* 1982;**243**:H1–12.
22. Menting ME, van den Bosch AE, McGhie JS, Eindhoven JA, Cuypers JAAE, Witsenburg M *et al.* Assessment of ventricular function in adults with repaired tetralogy of Fallot using myocardial deformation imaging. *Eur Heart J Cardiovasc Imaging* 2015;**16**:1347–57.
23. Dragulescu A, Grosse-Wortmann L, Redington A, Friedberg MK, Mertens L. Differential effect of right ventricular dilatation on myocardial deformation in patients with atrial septal defects and patients after tetralogy of Fallot repair. *Int J Cardiol* 2013;**168**:803–10.
24. Bodhey NK, Beerbaum P, Sarikouch S, Kropf S, Lange P, Berger F *et al.* Functional analysis of the components of the right ventricle in the setting of tetralogy of Fallot. *Circ Cardiovasc Imaging* 2008;**1**:141–7.
25. van der Hulst AE, Roest AAW, Holman ER, de Roos A, Blom NA, Bax JJ *et al.* Real-time three-dimensional echocardiography: segmental analysis of the right ventricle in patients with repaired tetralogy of Fallot. *J Am Soc Echocardiogr* 2011;**24**:1183–90.
26. Hui W, Slorach C, Dragulescu A, Mertens L, Bijnens B, Friedberg MK. Mechanisms of right ventricular electromechanical dyssynchrony and mechanical inefficiency in children after repair of tetralogy of Fallot. *Circ Cardiovasc Imaging* 2014;**7**:610–8.
27. Sanchez-Quintana D, Anderson RH, Ho SY. Ventricular myoarchitecture in tetralogy of Fallot. *Heart* 1996;**76**:280–6.
28. Tretter JT, Friedberg MK, Wald RM, McElhinney DB. Defining and refining indications for transcatheter pulmonary valve replacement in patients with repaired tetralogy of Fallot: contributions from anatomical and functional imaging. *Int J Cardiol* 2016;**221**:916–25.
29. Geva T, Sandweiss BM, Gauvreau K, Lock JE, Powell AJ. Factors associated with impaired clinical status in long-term survivors of tetralogy of Fallot repair evaluated by magnetic resonance imaging. *J Am Coll Cardiol* 2004;**43**:1068–74.